Bioorganic & Medicinal Chemistry Letters 23 (2013) 3389–3392

Contents lists available at SciVerse ScienceDirect

Bioorganic & Medicinal Chemistry Letters

journal homepage: www.elsevier.com/locate/bmcl

Radiosynthesis and evaluation of [^{11}C]EMPA as a potential PET tracer for orexin 2 receptors

Changning Wang, Christian K. Moseley, Stephen M. Carlin, Colin M. Wilson, Ramesh Neelamegam, Jacob M. Hooker *

Athinoula A. Martinos Center for Biomedical Imaging, Department of Radiology, Massachusetts General Hospital, Harvard Medical School, Building 149, 13th Street, Suite 2301, Charlestown, MA 02129, United States

ARTICLE INFO

Article history:
Received 12 February 2013
Revised 15 March 2013
Accepted 20 March 2013
Available online 2 April 2013

Keywords:
Orexin
EMPA
PET radiotracer
Brain
Carbon-11

ABSTRACT

EMPA is a selective antagonist of orexin 2 (OX_2) receptors. Previous literature with [^{3}H]-EMPA suggest that it may be used as an imaging agent for OX_2 receptors; however, brain penetration is known to be modest. To evaluate the potential of EMPA as a PET radiotracer in non-human primate (as a step to imaging in man), we radiolabeled EMPA with carbon-11. Radiosynthesis of [^{11}C]*N*-ethyl-2-(*N*-(6-methoxypyridin-3-yl)-2-methylphenylsulfonamido)-*N*-(pyridin-3-ylmethyl)acetamide ([^{11}C]EMPA), and evaluation as a potential PET tracer for OX_2 receptors is described. Synthesis of an appropriate non-radioactive *O*-desmethyl precursor was achieved from EMPA with sodium iodide and chlorotrimethylsilane. Selective O-methylation using [^{11}C]CH_3I in the presence of cesium carbonate in DMSO at room temp afforded [^{11}C]EMPA in 1.5–2.5% yield (non-decay corrected relative to trapped [^{11}C]CH_3I at EOS) with ⩾95% chemical and radiochemical purities. The total synthesis time was 34–36 min from EOB. Studies in rodent suggested that uptake in tissue was dominated by nonspecific binding. However, [^{11}C]EMPA also showed poor uptake in both rats and baboon as measured with PET imaging.

The orexins are peptides that play an important role in the regulation of the sleep–wake cycle, modulating feeding behavior, and energy homeostasis.[1] A wide range of the central nervous system (CNS) disorders are associated with orexin receptors including insomnia,[2] cluster headache[3] and drug abuse.[4] Recent research also suggests that orexin receptors may be related or contribute to several disorders in peripheral organs.[5] Although they have diverse functions, orexin receptors have been most extensively investigated for their roles in the CNS and have been aggressively pursued as therapeutic targets for sleeping disorders.[6] The two members of the family, orexin-A (33 amino acids) and orexin-B (28 amino acids), are derived from the same biological precursor.[7] Two receptor subtypes, termed OX_1 and OX_2, have been identified.[8] Orexin-A is a nonselective neuropeptide that binds with similar affinities to OX_1 and OX_2 receptors, while orexin-B is a selective neuropeptide and has a 10-fold higher affinity for OX_2 over OX_1 receptors. Both receptors belong to the superfamily of G-protein-coupled receptors (GPCRs).[9]

Several small molecules have been reported as dual-OX_1 and OX_2 antagonists or selective OX_1 and OX_2 antagonists.[10] Due to the difference in affinity of OX_1 and OX_2 receptors over orexin-A and orexin-B, and the different distribution of OX_1 and OX_2 receptors, it is critically important to choose compounds that show a dramatic difference in affinity and efficacy between these subtypes. With this in mind, we selected EMPA for development of a PET radiotracer for orexin 2 receptors.[10d] EMPA is a selective antagonist at the OX_2 receptor (K_i = 1.10 ± 0.24 nM, OX_2: IC_{50} = 2 nM, OX_1: IC_{50} >10,000 nM). Previously, quantitative autoradiography has been used to determine the distribution and abundance of OX_2 receptors in rat brain (B_{max} = 6.62 ± 0.60 pmol mg^{-1} protein) with the tritium [^{3}H]-labeled EMPA.[10d] Selective binding in vitro to rat brain sections and ex vivo receptor occupancy studies revealed [^{3}H]-EMPA is a useful tool studying the pharmacology of OX_2. A high density of OX_2 receptors was observed in the CA3 region of the hippocampus, cortical layer 6, tuberomammillary nucleus, induseum griseum and nucleus accumbens in the rat brain using [^{3}H]-EMPA. The brain/plasma concentration ratio of EMPA determined at 45 min after ip administration was modest (0.7 in mouse), but sufficient for us to believe that synthesis and evaluation of [^{11}C]EMPA in rodents and non-human primates was warranted.

Syntheses of the nonradioactive standard, EMPA, and *O*-desmethyl precursor **1** were achieved in good yield starting from 6-methoxypyridin-3-amine (Scheme 1). 6-Methoxypyridin-3-amine was treated with 2-methylbenzene-1-sulfonyl chloride in pyridine to obtain *N*-(6-methoxypyridin-3-yl)-2-methylbenzenesulfonamide (**2**) in 88% yield. Compound **2** was coupled with methyl

* Corresponding author. Tel.: +1 617 726 6596; fax: +1 617 726 7422.
E-mail address: hooker@nmr.mgh.harvard.edu (J.M. Hooker).

0960-894X/$ - see front matter © 2013 Elsevier Ltd. All rights reserved.
http://dx.doi.org/10.1016/j.bmcl.2013.03.079

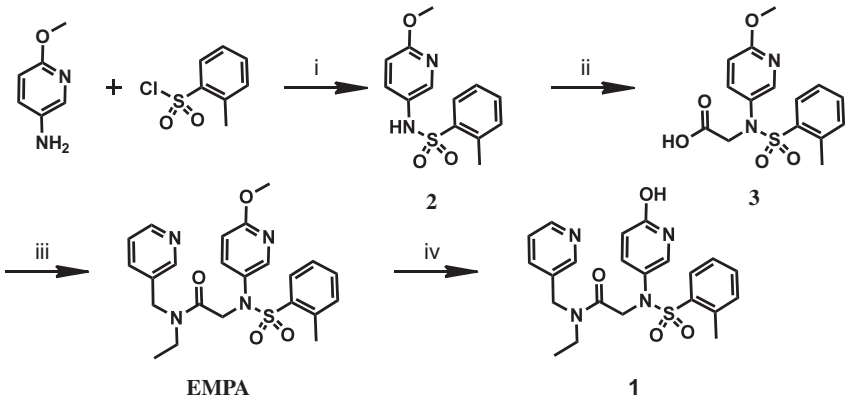

Scheme 1. Synthesis of EMPA and its precursor (**1**). Reagents and conditions: (i) pyridine, 0 °C to rt, 1 h, 88%; (ii) methyl bromoacetate, *t*BuOK, DMSO, 60 °C; 1 M NaOH aq, MeOH, 1 h, 80 °C, 63%; (iii) *N*-(pyridin-3-ylmethyl)ethanamine, EDC·HCl, DCM, 72%; and (iv) NaI, TMSCl, MeCN, reflux, 2 h, 75%.

2-bromoacetate. The resulting compound was then hydrolyzed with 1 M NaOH aq to form carboxylic acid **3**, which was then coupled to *N*-(pyridin-3-ylmethyl) ethanamine in the presence of EDC·HCl providing EMPA.[11] EMPA was treated with sodium iodide and chlorotrimethylsilane, refluxing in acetonitrile to obtain **1** as the O-desmethyl precursor.[12]

We anticipated two methylation sites on precursor **1** and indeed found that methylation with CH_3I in the presence of various bases in DMSO afforded a mixture of the N-methylated and O-methylated products. Reaction conditions to optimize for radiochemical O-methylation were evaluated using stochiometric amounts of CH_3I (1 equiv), precursor **1** (1 mg), and several bases. We found that the use of K_2CO_3 at 50 °C predominantly formed the N-methylated compound and anticipated that O-methylation would occur preferentially at lower temperatures. Based on our small screen of reaction conditions with precursor **1** and various bases at room temperature, we found Cs_2CO_3 yielded the greatest proportion of O-methylated product (Table 1). The N-methylated and O-methylated products could be separated by HPLC, which we used as our strategy to isolate [^{11}C]EMPA described below.

As shown in Scheme 2, precursor **1** reacted with [^{11}C]CH_3I in 0.3 mL DMSO in the presence of cesium carbonate at room temperature to provide [^{11}C]EMPA. The radiolabelled product was purified via semi-preparative C-18 HPLC (70% H_2O + TFA (0.1% v/v)/30% CH_3CN + TFA (0.1% v/v), 5.0 mL/min, the desired product was collected between 11 and 11.5 min) and the final product was reformulated by loading onto solid-phase exchange (SPE) C-18 cartridges rinsed with H_2O (5 mL), eluted with EtOH (1 mL), and diluted with saline (0.9%, 9 mL).[13] The average radiochemical yield

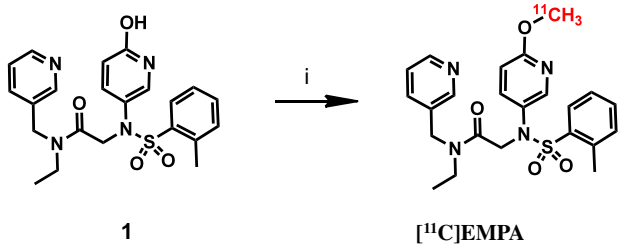

Scheme 2. Radiosynthesis of [^{11}C]EMPA. Reagents and conditions: (i) $^{11}CH_3I$, Cs_2CO_3, DMSO, rt, 3 min. RCY: 1.5–2.5% (decay-uncorrected to trapped [^{11}C]CH_3I). Specific acitivity: 100 ± 20 mCi/μmol.

was 1.5–2.5% (decay-uncorrected 1.5–2.5% yield at the end of synthesis (EOS, non-decay corrected relative to trapped [^{11}C]CH_3I) to trapped [^{11}C]CH_3I; $n = 3$). Chemical and radiochemical purities were ⩾95% with a specific activity ranged from 100 ± 20 mCi/μmol (end of bombardment, EOB).

With [^{11}C]EMPA available, we examined its lipophilicity[14] and plasma protein binding[15] in vitro. Both the log*D* (1.94, $n = 2$) and plasma protein binding (PPB, 11.33% unbound, $n = 3$) appeared suitable for blood–brain barrier (BBB) penetration. Given the literature precedence and our analysis of the physical properties of EMPA, including its molecular weight, lipophilicity, and PPB character, we anticipated that [^{11}C]EMPA may suitably cross the BBB for evaluation as an OX_2 imaging agent.

We first examined the BBB permeability of [^{11}C]EMPA by PET-CT scans in anesthetized male Sprague–Dawley (SD) rats.[16]

Table 1
Assessment of N-methylation to O-methylation selectivity for various reaction conditions

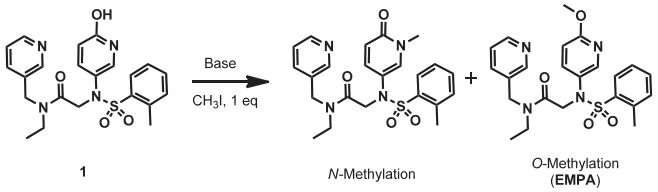

Bases	Time (min)	Temp (°C)	Solvent (300 μL)	N/O methylation ratio[a]
K_2CO_3 (5 mg)	3	50	DMF or DMSO	>99:1
Ag_2CO_3 (3 mg)	3	25	DMSO	2.5:1
1 M NaOH (10 μL)	3	25	MeOH or DMSO	>99:1
1 M TBA-OH (10 μL)	3	25	DMSO	2:1
Cs_2CO_3 (5 mg)	3	25	DMSO	1.3:1

[a] N/O methylation ratio was measured by HPLC.

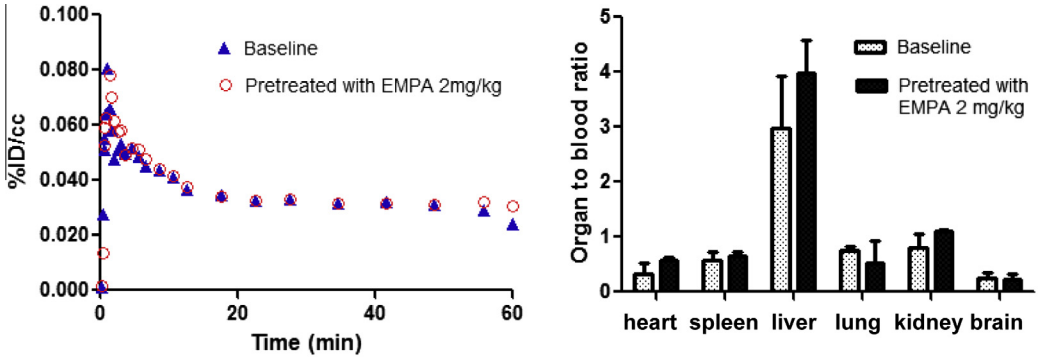

Figure 1. (A) Whole-brain time–activity curves generated from rodent PET imaging data (0–60 min). (B) Biodistribution of [^{11}C]EMPA in rats at 90 min post injection (gray) and following pretreatment with unlabeled EMPA (black). Data are normalized to blood (n = 2).

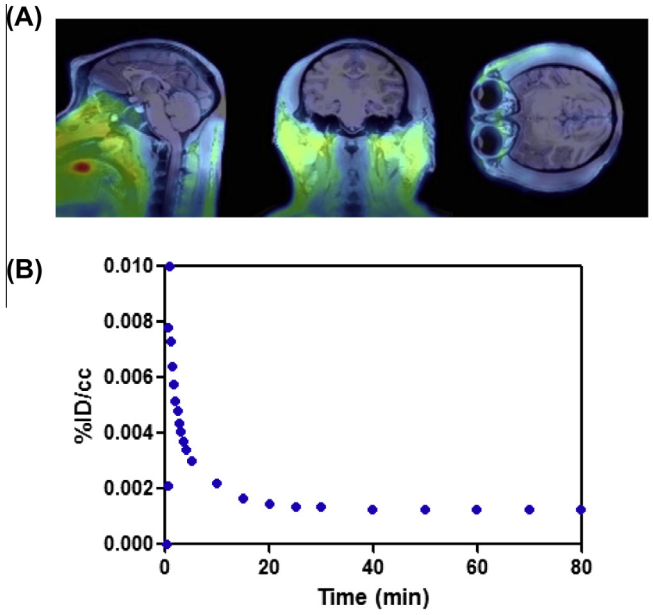

Figure 2. (A) [^{11}C]EMPA PET-MRI imaging (baboon brain). Summed PET images (0–80 min) superimposed with a MEMPRAGE-MRI of the brain from the same baboon, following injection of [^{11}C]EMPA (4.49 mCi). (B) Whole brain time–activity curve for [^{11}C]EMPA in baboon.

Anesthesia was performed with isoflurane. For saturability determination, we co-administered [^{11}C]EMPA and EMPA (2 mg/kg) to rats intravenously. The radiotracer was injected at the dose of 1.0–1.2 mCi for each study and emission data were collected for 60 min. A concentration of less than 0.1% of the injected dose per cubic centimeter was distributed in the brain tissue (Fig. 1). The organs of greatest accumulation were the liver and kidneys at 90 min (Fig. 1B), which is expected after metabolism and excretion of the radiotracer. We noted that whole brain uptake was not different with unlabeled EMPA pretreatment indicating [^{11}C]EMPA has high nonspecific binding in the rat brain.

To determine if the [^{11}C]EMPA has species-dependent brain permeability, we conducted the [^{11}C]EMPA PET-MR imaging in a *Papio anubis* baboon. [^{11}C]EMPA exhibited very poor BBB penetration and low brain uptake over the scanning time (80 min),[17] (Fig. 2). Coregistration of the PET image with an MRI of the same animal indicated that the areas appearing to have modest levels of radioactive uptake are in blood pool regions outside of the BBB,[18] and less than 0.01% of the injected dose per cubic centimeter was distributed in the brain tissue. One explanation of the failure of brain penetration of EMPA is that EMPA may be a permeability glycoprotein (P-gp) substrate that limit BBB penetration. Further in vitro and in vivo experiments will be required to investigate mechanisms, however this limits the potential of [^{11}C]EMPA as an OX_2 receptor imaging agent in humans.

In summary, we have successfully synthesized [^{11}C]EMPA by O-methylation and evaluated the potential for its use in human PET imaging. The total time required for the radiosynthesis was 34–36 min from EOB using [^{11}C]CH_3I and cesium carbonate in DMSO. Radiolabelled product was obtained in 1.5–2.5% yield (EOS) with excellent purity in the formulation. However, in vivo PET studies in rats and baboon showed poor uptake in brain. Our studies suggest that EMPA would not be a good PET tracer for neurological disorders diagnosis by targeting OX_2 receptor in the CNS and that new orexin imaging probes designed specifically for the CNS are needed.

Acknowledgments

This research was carried out at the Athinoula A. Martinos Center for Biomedical Imaging at the Massachusetts General Hospital, using resources provided by the Center for Functional Neuroimaging Technologies, P41EB015896, a P41 Regional Resource supported by the National Institute of Biomedical Imaging and Bioengineering (NIBIB), National Institutes of Health. This work also involved the use of instrumentation supported by the NIH Shared Instrumentation Grant Program and/or High-End Instrumentation Grant Program; specifically, Grant numbers: S10RR017208, S10RR026666, S10RR022976, S10RR019933, S10RR029495. We would like to thank members of the Hooker laboratory for helpful discussions. The authors are grateful to Joseph Mandeville, Grae Arabsz, Shirley Hsu, and Helen Deng for assistance during NHP imaging.

References and notes

1. Siegel, J. M. *Annu. Rev. Psychol.* **2004**, *55*, 125.
2. Dall'aglio, C.; Mercati, F.; Maranesi, M.; Boiti, C. *Peptides* **2012**, *35*, 36.
3. (a) Rainero, I.; Rubino, E.; Valfre, W.; Gallone, S.; De Martino, P.; Zampella, E.; Pinessi, L. *J. Headache Pain* **2007**, *8*, 152; (b) Rainero, I.; Gallone, S.; Rubino, E.; Ponzo, P.; Valfre, W.; Binello, E.; Fenoglio, P.; Gentile, S.; Anoaica, M.; Gasparini, M.; Pinessi, L. *Headache* **2008**, *48*, 1108.
4. (a) Scammell, T. E.; Saper, C. B. *Nat. Med.* **2007**, *13*, 126; (b) Nixon, J. P.; Kotz, C. M.; Novak, C. M.; Billington, C. J.; Teske, J. A. *Handb. Exp. Pharmacol.* **2012**, *209*, 77; (c) Li, Y.; Wang, H.; Qi, K.; Chen, X.; Li, S.; Sui, N.; Kirouac, G. J. *Physiol. Behav.* **2011**, *102*, 42.
5. (a) Silveyra, P.; Lux-Lantos, V.; Libertun, C. *Am. J. Physiol. Endocrinol. Metab.* **2007**, *293*, E977; (b) de Oliveira, C. V.; Rosas-Arellano, M. P.; Solano-Flores, L. P.; Ciriello, J. *Am. J. Physiol. Heart Circ. Physiol.* **2003**, *284*; (c) Ciriello, J.; Rosas-Arellano, M. P.; Solano-Flores, L. P.; de Oliveira, C. V. *Brain Res.* **2003**, *967*, 123; (d) Assisi, L.; Tafuri, S.; Liguori, G.; Paino, S.; Pavone, L. M.; Staiano, N.; Vittoria, A. *Cell Tissue Res.* **2012**; (e) Ehrstrom, M.; Gustafsson, T.; Finn, A.; Kirchgessner, A.; Gryback, P.; Jacobsson, H.; Hellstrom, P. M.; Naslund, E. *J. Clin. Endocrinol.*

Metab. **2005**, *90*, 2370; (f) Mazzocchi, G.; Malendowicz, L. K.; Aragona, F.; Rebuffat, P.; Gottardo, L.; Nussdorfer, G. G. *J. Clin. Endocrinol. Metab.* **2001**, *86*, 4818; (g) Spinazzi, R.; Rucinski, M.; Neri, G.; Malendowicz, L. K.; Nussdorfer, G. G. *J. Clin. Endocrinol. Metab.* **2005**, *90*, 3544; (h) Zwirska-Korczala, K.; Adamczyk-Sowa, M.; Sowa, P.; Pilc, K.; Suchanek, R.; Pierzchala, K.; Namyslowski, G.; Misiolek, M.; Sodowski, K.; Kato, I.; Kuwahara, A.; Zabielski, R. *J. Physiol. Pharmacol.* **2007**, *58*, 53; (i) Nakabayashi, M.; Suzuki, T.; Takahashi, K.; Totsune, K.; Muramatsu, Y.; Kaneko, C.; Date, F.; Takeyama, J.; Darnel, A. D.; Moriya, T.; Sasano, H. *Mol. Cell. Endocrinol.* **2003**, *205*, 43; (j) Takahashi, K.; Arihara, Z.; Suzuki, T.; Sone, M.; Kikuchi, K.; Sasano, H.; Murakami, O.; Totsune, K. *Peptides* **2006**, *27*, 871; (k) Ehrstrom, M.; Levin, F.; Kirchgessner, A. L.; Schmidt, P. T.; Hilsted, L. M.; Gryback, P.; Jacobsson, H.; Hellstrom, P. M.; Naslund, E. *Regul. Pept.* **2005**, *132*, 9.

6. (a) Brisbare-Roch, C.; Dingemanse, J.; Koberstein, R.; Hoever, P.; Aissaoui, H.; Flores, S.; Mueller, C.; Nayler, O.; van Gerven, J.; de Haas, S. L.; Hess, P.; Qiu, C.; Buchmann, S.; Scherz, M.; Weller, T.; Fischli, W.; Clozel, M.; Jenck, F. *Nat. Med.* **2007**, *13*, 150; (b) Whitman, D. B.; Cox, C. D.; Breslin, M. J.; Brashear, K. M.; Schreier, J. D.; Bogusky, M. J.; Bednar, R. A.; Lemaire, W.; Bruno, J. G.; Hartman, G. D.; Reiss, D. R.; Harrell, C. M.; Kraus, R. L.; Li, Y.; Garson, S. L.; Doran, S. M.; Prueksaritanont, T.; Li, C.; Winrow, C. J.; Koblan, K. S.; Renger, J. J.; Coleman, P. J. *ChemMedChem* **2009**, *4*, 1069; (c) Cox, C. D.; McGaughey, G. B.; Bogusky, M. J.; Whitman, D. B.; Ball, R. G.; Winrow, C. J.; Renger, J. J.; Coleman, P. J. *Bioorg. Med. Chem. Lett.* **2009**, *19*, 2997; (d) Malherbe, P.; Borroni, E.; Pinard, E.; Wettstein, J. G.; Knoflach, F. *Mol. Pharmacol.* **2009**, *76*, 618.
7. de Lecea, L.; Kilduff, T. S.; Peyron, C.; Gao, X.; Foye, P. E.; Danielson, P. E.; Fukuhara, C.; Battenberg, E. L.; Gautvik, V. T.; Bartlett, F. S., II; Frankel, W. N.; van den Pol, A. N.; Bloom, F. E.; Gautvik, K. M.; Sutcliffe, J. G. *Proc. Natl. Acad. Sci. U.S.A.* **1998**, *95*, 322.
8. Alexander, S. P.; Mathie, A.; Peters, J. A. *Br. J. Pharmacol.* **2008**, *153*, S1.
9. Sakurai, T.; Amemiya, A.; Ishii, M.; Matsuzaki, I.; Chemelli, R. M.; Tanaka, H.; Williams, S. C.; Richarson, J. A.; Kozlowski, G. P.; Wilson, S.; Arch, J. R.; Buckingham, R. E.; Haynes, A. C.; Carr, S. A.; Annan, R. S.; McNulty, D. E.; Liu, W. S.; Terrett, J. A.; Elshourbagy, N. A.; Bergsma, D. J.; Yanagisawa, M. *Cell* **1998**, *92*, 1.
10. (a) Cole, A. G.; Stroke, I. L.; Qin, L. Y.; Hussain, Z.; Simhadri, S.; Brescia, M. R.; Waksmunski, F. S.; Strohl, B.; Tellew, J. E.; Williams, J. P.; Saunders, J.; Appell, K. C.; Henderson, I.; Webb, M. L. *Bioorg. Med. Chem. Lett.* **2008**, *18*, 5420; (b) Perrey, D. A.; Gilmour, B. P.; Runyon, S. P.; Thomas, B. F.; Zhang, Y. *Bioorg. Med. Chem. Lett.* **2011**, *21*, 2980; (c) Langmead, C. J.; Jerman, J. C.; Brough, S. J.; Scott, C.; Porter, R. A.; Herdon, H. J. *Br. J. Pharmacol.* **2004**, *141*, 340; (d) Malherbe, P.; Borroni, E.; Gobbi, L.; Knust, H.; Nettekoven, M.; Pinard, E.; Roche, O.; Rogers-Evans, M.; Wettstein, J. G.; Moreau, J. L. *Br. J. Pharmacol.* **2009**, *156*, 1326.
11.. EMPA: 1H-NMR (500 MHz, CDCl3): δ 8.44 (d, J = 4.5 Hz, 1H), 8.35 (s, 1H), 7.94 (d, J = 2.0 Hz, 1H), 7.74 (d, J = 8.0 Hz, 1H), 7.55 (m, 1H), 7.38 (m, 2H), 7.17 (m, 3H), 6.58 (d, J = 8.5 Hz, 1H), 4.53 (s, 2H), 4.46 (s, 2H), 3.84 (s, 3H), 3.27 (q, 2H), 2.44 (s, 3H), 1.12 (t, J1 = J2 = 7.0 Hz, 3H). 13C-NMR (125 MHz, CDCl3): δ 167.0, 163.3, 149.2, 148.9, 147.8, 140.0, 138.2, 136.5, 135.5, 133.1, 132.8, 132.6, 130.4, 129.7, 126.0, 123.4, 110.8, 53.6, 52.5, 46.2, 41.5, 20.6, 13.8. LC-MS calcd for C23H26N4O4S (M): 454.2; Found (M+1): 455.4.
12. *Precursor* **1**: ^{1}H NMR (500 MHz, DMSO-d_6): δ 8.73 (d, J = 8.5 Hz, 2H), 8.11 (d, J = 7.0 Hz, 1H), 7.83 (s, 1H), 7.76 (d, J = 8.0 Hz, 1H), 7.56 (m, 1H), 7.37 (m, 2H), 7.28 (m, 2H), 6.21 (d, J = 10 Hz, 1H), 4.69 (s, 2H), 4.63 (s, 2H), 3.36 (q, 2H), 2.51 (s, 3H), 1.10 (t, $J_1 = J_2$ = 7.0 Hz, 3H). ^{13}C NMR (125 MHz, DMSO-d_6): δ 168.3, 161.7, 143.3, 143.1, 142.1, 138.2, 137.7, 137.4, 133.7, 133.2, 130.3, 126.9, 126.8, 126.3, 119.6, 119.5, 119.0, 52.5, 46.1, 42.2, 20.6, 14.3. LC–MS calcd for $C_{22}H_{24}N_4O_4S$ expected (M): 440.2; found (M+1): 441.3.
13. $^{11}CO_2$ was obtained via the ^{14}N (p, α) ^{11}C reaction on nitrogen with 2.5% oxygen, with 11 MeV protons (Siemens Eclipse cyclotron), and trapped on molecular sieves in a TRACERlab FX-MeI synthesizer (General Electric). $^{11}CH_4$ was obtained by the reduction of $^{11}CO_2$ in the presence of Ni-hydrogen at 350 °C and passed through an oven containing I_2 to produce $^{11}CH_3I$ via a radical reaction. $^{11}CH_3I$ was trapped in a TRACERlab FX-M synthesizer reactor (General Electric) preloaded with a solution of precursor (**3**) (1.0 mg) and Cs_2CO_3 (6.0 mg) in dry DMSO (300 μL) that had stirred at rt for 5 min prior to trapping. The solution was stirred at rt for 3 min and water (1.2 mL) was added. The reaction mixture was purified by reverse phase semi-preparative HPLC (Phenomenex Gemini NX-C18, 250 × 10 mm, 5 μm, 5.0 mL/min, 70% H_2O + TFA (0.1% v/v)/30% CH_3CN + TFA (0.1% v/v)) and the desired fraction was collected. The final product was reformulated by loading onto a solid-phase exchange (SPE) C-18 cartridge rinsing with H_2O (5 mL), eluting with EtOH (1 mL), and diluting with saline (0.9%, 9 mL). The chemical and radiochemical purity of the final product was tested by analytical HPLC (Agilent Eclipse XDB-C18, 150 × 4.6 mm, 1.0 mL/min, 70% H_2O + TFA (0.1% v/v)/30% CH_3CN + TFA (0.1% v/v)). The identity of the product was confirmed by analytical HPLC with additional co-injection of EMPA reference standard. The average time required for the synthesis from end of cyclotron bombardment to end of synthesis was 34–36 min. The average radiochemical yield was 1.5–2.5% (decay-uncorrected to trapped [^{11}C]CH_3I; n = 3). Chemical and radiochemical purities were ⩾95% with a specific activity range from 100 ± 20 mCi/μmol (EOB).
14. *log D Determination:* An aliquot (~50 μL) of the formulated [^{11}C]EMPA was added to a test tube containing 2.5 mL of octanol and 2.5 mL of phosphate buffer solution (pH 7.4). The test tube was mixed by vortex for 2 min and then centrifuged for 2 min to fully separate the aqueous and organic phase. A sample taken from the octanol layer (0.1 mL) and the aqueous layer (1.0 mL) was saved for radioactivity measurement. An additional aliquot of the octanol layer (2.0 mL) was carefully transferred to a new test tube containing 0.5 mL of octanol and 2.5 mL of phosphate buffer solution (pH 7.4). The previous procedure (vortex mixing, centrifugation, sampling, and transfer to the next test tube) was repeated until six sets of aliquot samples had been prepared. The radioactivity of each sample was measured in a WIZARD Automatic Gamma Counter (Perkin–Elmer, Waltham, MA).The log D of each set of samples was derived by the following equation: log D = log(decay-corrected radioactivity in octanol sample × 10/decay-corrected radioactivity in phosphate buffer sample).
15. *Plasma protein binding assay:* An aliquot of [^{11}C]EMPA in saline (10 μL) was added to a sample of baboon plasma (0.8 mL, pooled from two separate animals). The mixture was gently mixed by repeated inversion and incubated for 10 min at room temperature. Following incubation a small sample (20 μL) was removed to determine the total radioactivity in the plasma sample (A_T; $A_T = A_{bound} + A_{unbound}$). An additional 0.2 mL of the plasma sample was placed in the upper compartment of a centrifree tube (Amicon, Inc., Beverly, MA) and then centrifuged for 10 min. The upper part of the centrifree tube was discarded, and an aliquot (20 μL) from the bottom part of the tube was removed to determine the amount of radioactivity that passed through the membrane ($A_{unbound}$). Plasma protein binding was derived by the following equation: %unbound = $A_{unbound} \times 100/A_T$.
16. *Rodent PET/CT acquisition:* Male Sprague–Dawley rats were utilized in pairs, anesthetized with inhalational isoflurane (Forane) at 3% in a carrier of 2 L/min medical oxygen and maintained at 2% isoflurane for the duration of the scan. The rats were arranged head-to-head in a Triumph Trimodality PET/CT/SPECT scanner (Gamma Medica, Northridge, CA) featuring a PET resolution of approximately 1 mm. Rats were injected with standard references or vehicle via a lateral tail vein catheterization at the start of PET acquisition. Dynamic PET acquisition lasted for 60–90 min and was followed by computed tomography (CT) for anatomic coregistration.
17. *Baboon MR-PET acquisition:* A female *Papio Anubis* baboon, deprived of food for 12 h prior to the study, was administered intramuscular ketamine (10 mg/kg) and intubated. For maintenance of anesthesia throughout the study, the baboon was provided 1–4% isoflurane (Forane) in a mixture of medical oxygen and nitrogen. The baboon was catheterized antecubitally for radiotracer injection and a radial arterial line was placed for metabolite analysis. MR-PET images were acquired in a Biograph mMR scanner (Siemens, Munich, Germany), with a PET resolution of 5 mm and field of view of 59.4 and 25.8 cm (transaxial and axial, respectively). Dynamic PET image acquisition was initiated followed by administration of the radiotracer in a homogenous solution of 10% ethanol and 90% isotonic saline. An MEMPRAGE sequence began after 30 min of the baseline scan for anatomic coregistration. 4–5 mCi of [^{11}C] EMPA was administered to the baboon for each scan.
18. *Image reconstruction and analysis:* Dynamic data from the PET scans were recorded in list mode and corrected for attenuation. Baboon data were reconstructed using a 3D-OSEM method resulting in a full width at half-maximum resolution of 4 mm. Rat PET data were reconstructed using a 3D-MLEM method resulting in a full width at half-maximum resolution of 1 mm. Reconstructed images were exported from the scanner in DICOM format along with an anatomic CT for rodent studies and MRI for baboon scans. These files were imported to PMOD (PMOD Technologies, Ltd) and manually coregistered using six degrees of freedom. Volumes of interest (VOIs) were drawn manually as spheres in brain regions guided by high resolution structural images (MRI for baboon and CT for rats) and summed PET data, with a radius no less than double that of the PET voxel size to minimize partial volume effects (4 mm for baboon and 1 mm for rodent scans). A common VOI mask was applied to both baboon scans. Time–activity curves (TACs) were exported in terms of decay corrected activity per unit volume at specified time points with gradually increasing intervals. The TACs were expressed as percent injected dose per unit volume for analysis.